arXiv:1004.1002v1 [astro-ph.CO] 7 Apr 2010

The Correlations between the Intrinsic Colors and Spectroscopic Metallicities of M31 Globular Clusters

Zhou Fan[1,2], Jun Ma[1,2], Xu Zhou[1,2] and Zhaoji Jiang[1,2]

`zfan@nao.cas.cn`

ABSTRACT

We present the correlations between the spectroscopic metallicities and ninety-three different intrinsic colors of M31 globular clusters, including seventy-eight BATC colors and fifteen SDSS and near infrared $ugriz$K colors. The BATC colors were derived from the archival images of thirteen filters (from c to p), which were taken by Beijing-Arizona-Taiwan-Connecticut (BATC) Multicolor Sky Survey with a 60/90 cm f/3 Schmidt telescope. The spectroscopic metallicities adopted in our work were from literature. We fitted the correlations of seventy-eight different BATC colors and the metallicities for 123 old confirmed globular clusters, and the result implies that correlation coefficients of twenty-three colors $r > 0.7$. Especially, for the colors $(f-k)_0$, $(f-o)_0$, and $(h-k)_0$, the correlation coefficients are $r > 0.8$. Meanwhile, we also note that the correlation coefficients (r) approach zero for $(g-h)_0$, $(k-m)_0$, $(k-n)_0$, and $(m-n)_0$, which are likely to be independent of metallicity. Similarity, we fitted the correlations of metallicity and $ugriz$K colors for 127 old confirmed GCs. The result indicates that all these colors are metal-sensitive ($r > 0.7$), of which $(u\text{–K})_0$ is the most metal-sensitive color. Our work provides an easy way to simply estimate the metallicity from colors.

1. Introduction

Globular clusters (hereafter GCs) are the oldest bound stellar systems in the Milky Way and other galaxies. They provide a fossil record of the earliest stages of galaxy formation

---

[1] National Astronomical Observatories, Chinese Academy of Sciences, A20 Datun Road, Chaoyang District, Beijing 100012, China

[2] Key Laboratory of Optical Astronomy, National Astronomical Observatories, Chinese Academy of Sciences

and evolution. Located at a distance of ~ 780 kpc (Stanek & Garnavich 1998; Macri 2001) away, Andromeda (M31) is the nearest large spiral galaxy in our local group. According to the latest RBC v.4.0 (Galleti et al. 2004, 2006, 2007), M31 contains more than one thousand GCs and candidates. Therefore M31 GCs provide us an ideal laboratory for us to study the nature of extragalactic GCs and to better understand the formation and evolution of M31. Furthermore, since M31 is Sb-type, which is similar to our Galaxy, it may offer us the clues to formation and evolution history of our Galaxy.

The correlation of metallicity and colors of globular clusters has been previously studied by many authors: Brodie & Huchra (1990) fitted the correlations of metallicities and ($V-$K), ($J-$K) for Galactic GCs and applied the calibrated relation to M31 GCs to derive the metallicities of M31 GCs. Barmby et al. (2000) analyzed the correlations of ten intrinsic colors ($(B-V)_0$, $(B-R)_0$, $(B-I)_0$, $(U-B)_0$, $(U-V)_0$, $(U-R)_0$, $(V-R)_0$, $(V-I)_0$, $(J-\mathrm{K})_0$, $(U-\mathrm{K})_0$) and metallicity of 88 Galactic GCs. They find that the correlation coefficients r for all these ten colors range from 0.91 to 0.77, of which $(U-R)_0$ is the best metallicity indicator while $(V-R)_0$ is not so good. The authors also studied the $(J-\mathrm{K})_0$ and $(V-\mathrm{K})_0$ color-metallicity correlations for M31 and Milky Way globular clusters. In this work, we attempt to find the most metal-sensitive colors, which could be used for the derivation of the metallicities of GCs in the future work. It is well known that, spectroscopy is relatively expensive in terms of observational time and is rarely available for many extragalactic globular clusters. Hence it is useful to determine metallicities from photometry.

The studies on identification, classification and analysis of the M31 GCs have been started since the pioneering work of Hubble et al. (1932), (see e.g. Vetesnik 1962; Sargent et al. 1977; Battistini et al. 1980, 1987, 1993; Crampton et al. 1985; Barmby et al. 2000). These studies provided a large amount of photometric data in different photometric systems, i.e. CCD photometry, photoelectric photometry, and photographic plates, even visual photometry. In order to obtain homogeneous photometric catalogue of M31 GCs, Galleti et al. (2004, 2006, 2007) took the photometry of Barmby et al. (2000) as reference and transformed others to this reference and compiled the famous The Revised Bologna Catalogue of M31 GCs and GC candidates (The latest version is RBC v.4.0), where 654 confirmed GCs and 619 GC candidates of M31 have been included, and 772 former GC candidates have been proved to be stars, asterism, galaxy, region HII or extended cluster. The catalogue also includes the newly discovered star clusters from Mackey et al. (2006), Kim et al. (2007) and Huxor (2008). Mackey et al. (2006) reported the discovery of eight remote GCs in the outer halo of M31 by using the deep ACS images; Kim et al. (2007) found 1164 GCs and GC candidates in M31 with KPN 0.9 m telescope and the WIYN 3.5 m telescope, of which 559 are previously known GCs and 605 are newly found GC candidates; later, Huxor (2008) detected 40 new GCs in the halo of M31 with Isaac Newton Telescope and Canada-France-Hawaii Telescope data. Recently, Caldwell et al. (2009) presented a new catalogue of 670 likely star clusters, stars, possible stars and galaxies in the field of M31, all with updated high-quality coordinates being accurate to $0.2''$ based on the images from the Local Group Survey (Massey et al. 2006) or Digitized Sky Survey (DSS). Very recently, Peacock et al. (2010) identified M31 GCs with images from Wide Field CAMera (WFCAM) on the UK Infrared Telescope and SDSS archives, and performed the photometry for them in SDSS *ugriz* and infrared K bands. Furthermore, the authors combined all the identifications and photometry of M31 GCs from references and those of their new work and updated the M31 star cluster catalog, including 416 old confirmed clusters, 156 young clusters and 373 candidate clusters. Our work is based on the 416 old confirmed M31 GCs, from which we will select our sample GCs.

Studies of M31 GCs based on BATC observations are also numerous: Jiang et al. (2003) presented the BATC photometry of 172 GCs in the central ~ 1 deg^2 region of M31 and estimated the ages for them with the Simple Stellar Population (SSP) models. After that, Fan et al. (2009) added six more new BATC observations fields surrounding the central region and performed the photometry for thirty GCs, which did not have the broadband photometry before. With the photometry, the authors, for the first time, suggested the blue tilt of M31 GCs. Ma et al. (2009) fitted the ages of thirty-five GCs of the central M31 field which were not included in Jiang et al. (2003) with BATC, 2MASS and GALEX data and the SSP models. Later, Wang et al. (2010) performed the photometry for another 104 GCs of M31 and estimated the ages by fitting the SEDs with SSP models, revealing the existence of young, the intermediate-age and the old populations in M31.

In this paper, first we used the BATC data to analyze the correlations of spectroscopic metallicities and the colors of M31 GCs. Moreover, we did the similar work with the *ugriz*K band data. The paper is organized as follows: Sect. 2 describes the data utilized in our work, including the spectroscopic metallicity from literature, BATC archival images and the data reduction, the *ugriz*K photometry from literature, along with the reddening of M31 GCs. Sect. 3 present the analysis and the results on the correlations of the metallicities and intrinsic colors for M31 GCs. The summary and remarkable conclusions of our work are in Sect. 4.

2. Data

2.1. The Spectroscopic Metallicities Adopted

The spectroscopic metallicities used in our analysis were from Perrett et al. (2002), who measured the metallicites for over 200 GCs in M31 with William Herschel 4.2 m telescope in

La Palma, Canary Islands from Nov. 3 to 6, 1996. The Wide Field Fibre Optic Spectrograph (WYFFOS) and two gratings (the H2400B 2400 line grating and the R1200R 1200 line grating) were applied for the observations. The dispersion of H2400B 2400 line grating is 0.8 Å pixel^{-1} and spectral resolution is 2.5 Å over the range $3700-4500$ Å. The dispersion of the R1200R 1200 line grating observations is 1.5 Å pixel^{-1} and the resolution is 5.1 Å over the spectral range $4400-5600$ Å. The total wavelength coverage of the spectra is $\sim 3700-5600$ Å, and it can coverage the spectral features such as CN, Hβ, the Mg b triplet, iron lines. For homogenous reason, we only adopted the spectroscopic metallicities from Perrett et al. (2002) in our work.

2.2. The BATC Archival Images and Photometry

The 15-band archival images of M31 field were obtained by BATC 60/90cm f/3 Schmidt telescope at Xinglong site of Hebei Provence, China, during 1995 February – 2008 March. The total exposure time of archival M31 BATC images is 143.9 hours with 447 frames and covering $\sim$ 6 deg^2 sky field. The observations and dataset are described in detail by Fan et al. (2009). The fifteen intermediate-band filters of BATC system are specifically designed to avoid most bright night-sky emissions, covering the wavelength range of ∼3,000 to ∼10,000 Å (see e.g. Fan et al. 1996; Yan et al. 2000; Zhou et al. 2003; Fan et al. 2009; Ma et al. 2009).

Before this work, Fan et al. (2009) have performed usual data reduction for these images, including bias subtraction and flat fielding of the CCD images, with an automatic data-reduction routine PIPELINE I, developed for the BATC sky survey based on IRAF. The BATC magnitudes are well defined and obtained in a similar way as for the spectrophotometric AB magnitude system (for details see Yan et al. 2000; Zhou et al. 2003; Ma et al. 2009). For BATC fifteen intermediate-band filters $abcdefghighmnop$ of the central field of M31 (M31-1 field), Fan et al. (2009) calibrated the combined images with Oke & Gunn (1983) standard stars (see e.g. Fan et al. 1996; Yan et al. 2000; Zhou et al. 2003), while for the M31-2 to M31-7 fields, the secondary standard stars of the overlapping field were used for the flux calibration (for details see Fan et al. 2009).

In this work, we performed the aperture photometry for M31 GCs with the BATC photometric routine PIPELINE II, which is the revised version of IRAF *daofind* and *daophot* for BATC system data reduction. For aperture photometry parameters, we adopted the aperture radius $r = 5''.1$ and the inner sky radius and outer sky radius are $\sim 13''.6$ and $\sim 22''.1$, respectively, which are the same parameters as those used in Jiang et al. (2003); Fan et al. (2009); Ma et al. (2009); Wang et al. (2010) for consistency. After careful checking all the images, we found the signal-to-noise ratios (SNR) of BATC a-band and b-band images are not high enough for our study, thus we do not included these images in the following work. Then, we obtained the BATC magnitudes of our sample GCs in the thirteen bands (from c to p), covering the wavelength from $\sim 4,000$ to $\sim 10,000$ Å.

Because the spectroscopic metallicities of Perrett et al. (2002) were based on the [Fe/H] calibration of Brodie & Huchra (1990), who only included old GCs in their calibration sample, only the metallicities of the old GCs in Perrett et al. (2002) are reliable. Further, it has long been known that the degeneracy of age and metallicity for SEDs and color fitting of the star clusters (see e.g. Worthey 1994; Jiang et al. 2003; Fan et al. 2006; Ma et al. 2007). However, fortunately, the SED/colors are only weakly correlated with age, if the GCs are old enough. Thus, if we only study the old GCs, the SED/colors are only a function of metallicity, which could eliminate effects of the other factors. For these reasons, we just used the old confirmed GCs with observed metallcities to avoid these problems and ensure our results reliable. This resulted in 144 matches between the the sample of 416 old confirmed clusters from Peacock et al. (2010) and the spectroscopic metallicity sample of Perrett et al. (2002). All the matched M31 GCs are shown in Fig. 1 with BATC observational field overlaid. The matched GCs are marked with small circles, of which four are out of BATC field of view.

For the comparisons with the previous photometry of these M31 GCs, we transformed the BATC intermediate-band system to the $UBVRI$ broad-band system using the transformation formulas between these two systems from Zhou et al. (2003). The formulas were derived based on the BATC observations of the Landolt standard stars from the catalogs of Landolt (1983, 1992) and Galadí-Enríquez et al. (2000) in fifteen colors. Since the photometry in the BATC a and b filters are not used in our work, we cannot obtain the U magnitudes from BATC photometry. Fig. 2 shows the comparisons of the B, V, R, and I photometry in our work with previous measurements from RBC v.4.0. The mean magnitude offsets are $\overline{B_{BATC} - B_{RBC}} = -0.08 \pm 0.20$, $\overline{V_{BATC} - V_{RBC}} = -0.08 \pm 0.30$, $\overline{R_{BATC} - R_{RBC}} = 0.14 \pm 0.35$, $\overline{I_{BATC} - I_{RBC}} = 0.04 \pm 0.19$. From this figure it can be seen that the B, V and I derived from BATC photometry are consistent with that from RBC v.4.0, although there are some scatter points. It also might be noticed that the offset of the R-band photometry is slightly larger than that for the other band. This may be due to the errors in the transformation formula by using the BATC photometry of the Landolt standard stars, since the spectrum of a globular cluster and a star is different. Further, we should be aware of heterogeneous photometry summarized in RBC v.4.0 although the authors made great effort to make it uniform, which might still introduce the offset in the comparisons. In general, we believe that our photometry is consistent with the previous studies and it will not produce bias or affect our results in our work.

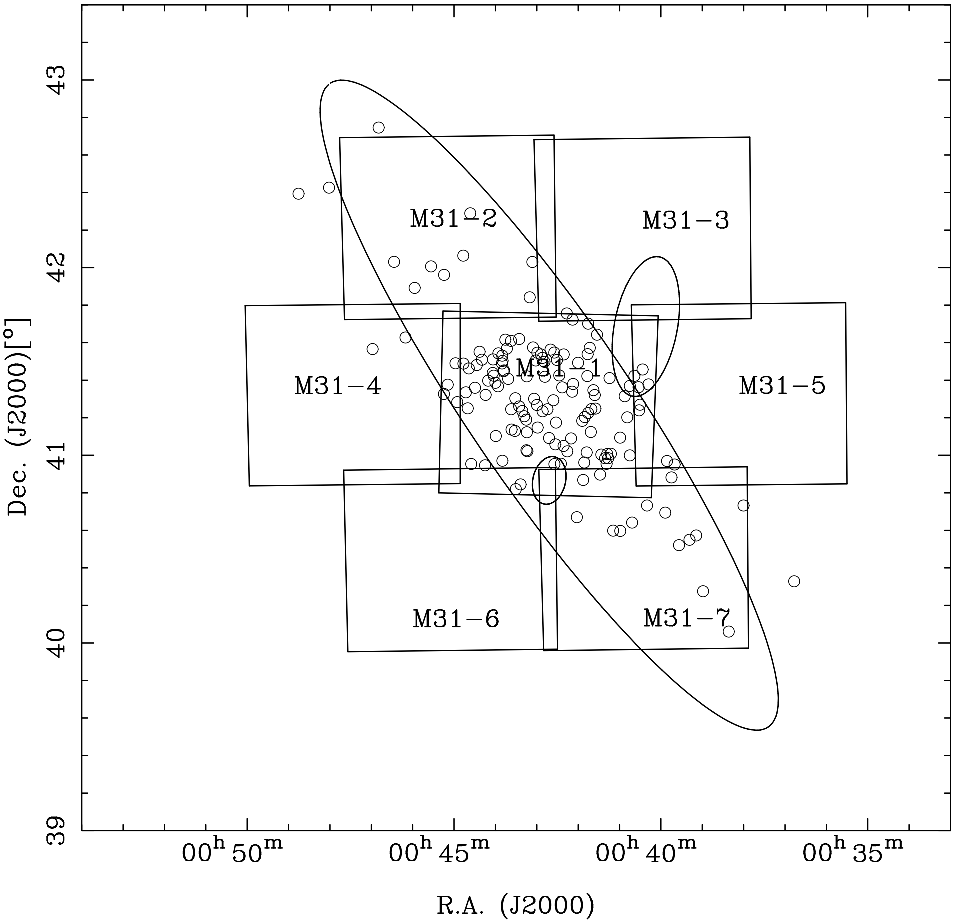

Fig. 1.— The spatial distribution of our sample of M31 GCs represented with small circles. The big ellipse marked the boundary of M31 disk (Racine 1991) while the other two small ellipses are D_{25} of NGC 205 (northwest) and M32 (southeast), respectively. The seven large boxes represent the seven observational fields of BATC imaging survey. The angular size of each BATC imaging field is $\sim 58' \times 58'$. North is up and east is to the left.

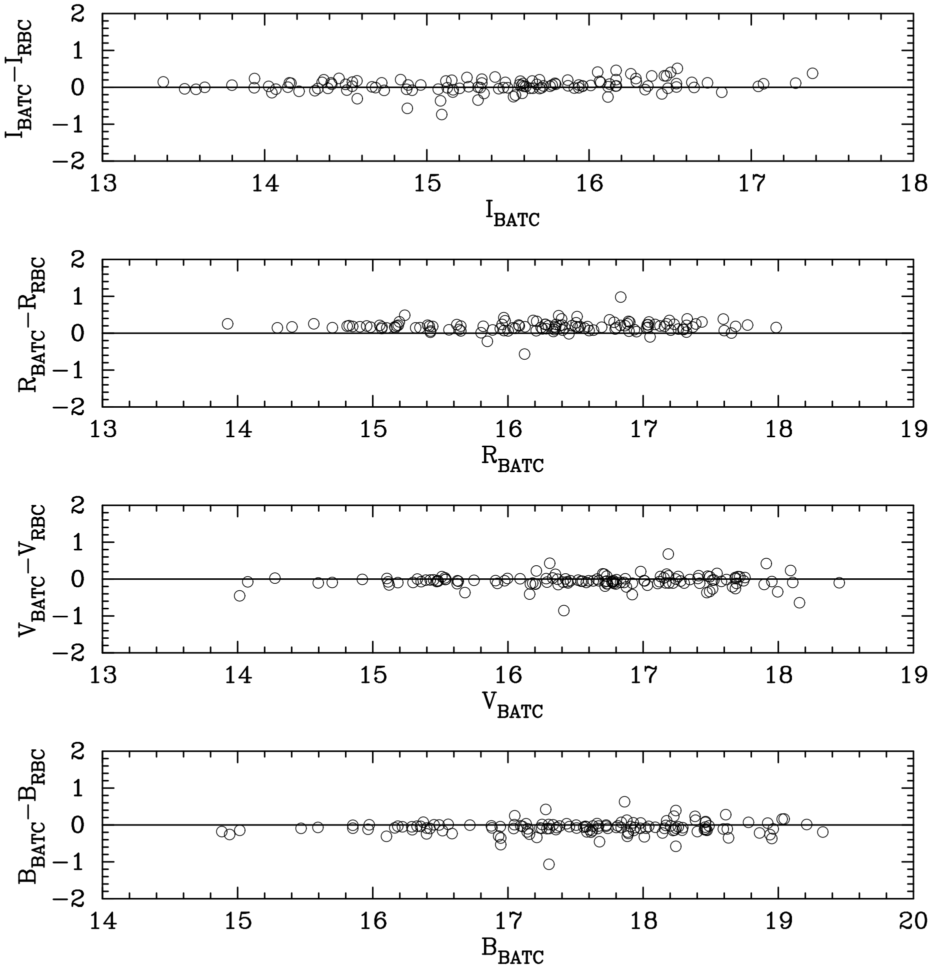

Fig. 2.— The comparisons of broadband magnitudes from BATC and those from RBC v.4.0. The mean magnitude offsets are $\overline{B_{BATC} - B_{RBC}} = -0.08 \pm 0.20$, $\overline{V_{BATC} - V_{RBC}} = -0.08 \pm 0.30$, $\overline{R_{BATC} - R_{RBC}} = 0.14 \pm 0.35$, $\overline{I_{BATC} - I_{RBC}} = 0.04 \pm 0.19$. The figure indicates that the our photometry are basically consistent with the previous photometry from RBC v.4.0.

2.3. The *ugriz*K Photometry from literature

As we described in Sect. 1, Peacock et al. (2010) identified M31 GCs with the SDSS archive and images taken from Wide Field CAMera (WFCAM) on the UK Infrared Telescope. The authors used the SExtractor (Bertin & Arnouts 1996) for the identifications and photometry of sources in SDSS images and they found good consistency with the previous photometry. The K-band images were reduced with the WFCAM pipeline and the magnitudes were calibrated with the 2MASS Point Source Catalogue. Thus, we draw the attention of readers that the *ugriz* photometry of Peacock et al. (2010) is in AB-based photometric system while for the K photometry is in Vega-based photometric system. In our work, we did not transform all the magnitudes into the same (AB-based or Vega-based) photometric system because such color shift will not affect the correlations coefficients in our analysis. Further this way could keep consistency and avoid confusion. Finally the authors listed the photometry for 416 old confirmed M31 GCs in the SDSS *ugriz* bands and 2MASS K band, which may be the latest work for study of M31 GCs. This photometry catalogue will be utilized for our following analysis.

2.4. The Reddenings of M31 GCs

In order to obtain the intrinsic colors for the sample GCs, all the colors derived in our work should be corrected by reddening. Here we adopted the reddening from Barmby et al. (2000) and Fan et al. (2008), which are the two most comprehensive reddening catalogue for M31 GCs so far. Barmby et al. (2000) calibrated the relations of the intrinsic color and metallicity and the $Q-$parameters for the Galactic GCs and then applied the relations to M31. The authors assumed that the extinction laws of M31 and Milky Way are the same, and they proved that the assumption is reasonable, which indicates their results are reliable. Finally, Barmby et al. (2000) determined the reddenings for 314 of M31 GCs and GC candidates, of which 221 are reliable (from the private communication). Later, Fan et al. (2008) used the similar method with the photometry of RBC v.3.5 (Galleti et al. 2004) and enlarged the reddening sample of M31 GCs to 443 ones, half of which have $E(B-V) \leq 0.2$. Moreover, Fan et al. (2008) find good agreement between their reddening with the previously determined reddening of Barmby et al. (2000). These two reddening catalogues of M31 GCs will be applied for our following study.

3. Analysis and Results

In this section, we investigate the correlations between spectroscopic metallicities and the BATC colors; further we analyzed the similar correlations for *ugriz*K colors in Peacock et al. (2010). The main goal of this paper is to find the most metal-sensitive and most metal-nonsensitive colors, which might provide a method for roughly estimating the metallicities just by colors.

3.1. The Correlations of BATC colors and metallicities

From the 140 GCs in the BATC field of Fig. 1, there are still nine clusters which we cannot obtain accurate photometric measurements due to nearby bright objects (B065-G126, B091D-D058, B160-G214 and B072), very low signal-to-noise (B305-D024), or steep gradients in the galaxy light near the nucleus (B129). Moreover, there are some problems with the photometry of three GCs: B127-G185, B225-G280 and B306-G029. We found "emission lines" in their SEDs, however, after careful checking of images, it turns out to be not real. For these reasons, we exclude these nine clusters from our sample and reduce the number of sample GCs to 131, which have the reliable BATC photometry.

Because we only concern the intrinsic colors, all the observed colors obtained in our work are required to be corrected by reddening. As recalled in Sect. 2.4, the reddening of M31 GCs from Fan et al. (2008) and Barmby et al. (2000) will be applied for the estimation of intrinsic colors. For each object, we searched and adopted the reddening from Fan et al. (2008) as priority, since it is homogeneous and the number of GCs included is greater than that of Barmby et al. (2000). If a GC does not have the reddening in Fan et al. (2008), we used the reddening of Barmby et al. (2000) instead. Considering the reddening can affect the color (hence the correlations) significantly, the GCs which do not have reddenings from either Fan et al. (2008) or Barmby et al. (2000) are excluded from our analysis. After the elimination, we obtain 123 old confirmed GCs with known reddening, which will be used as our final sample for the analysis of correlations between the metallicity and BATC colors.

As discussed in Sect. 2.2, the images in the thirteen BATC bands (from c to p band) were used in our work, thus seventy-eight different colors could be derived and used in the correlations analysis. We plotted the correlations between all the BATC intrinsic color and the metallicities from Perrett et al. (2002) in Fig.3. We performed the linear regressions of the intrinsic colors against metallicity correlations for the 123 GCs of M31 with an equation below,

$$(x-y)_0 = a + b[\mathrm{Fe/H}] \tag{1}$$

Here we use $(x-y)_0$ as general notation to represent any intrinsic BATC color. It is worth noting that there are several outliers in Fig.3, which seems not to follow the general trend very well. This may be due to the errors on the metallicity, inaccurate reddening estimates, or the errors on the photometry. Further, although the GCs in our sample are old and the SEDs almost the same, the slight difference of ages also might cause such scatter.

Table 1 lists the BATC intrinsic colors, intercede a and slope b, the correlation coefficients r, fitting point numbers of our sample of M31 GCs. Finally, we find that correlation coefficients of 23 colors $r > 0.7$. In particular, even for the colors $(f-k)_0$, $(f-o)_0$, $(h-k)_0$, the correlation coefficients $r > 0.8$. These metal-sensitive colors could be used for estimating the metallicity in the future work. However, it should also be noted that the correlation coefficients approach zero for $(g-h)_0$, $(k-m)_0$, $(k-n)_0$, $(m-n)_0$, which are nearly independent of metallicity. This result can be explained by there being less absorption lines in the corresponding wavelength span.

3.2. The Correlations of *ugriz*K colors and metallicities

Similar to the procedure in Sect. 3.1, in the following section, we will analyze the correlations between SDSS *ugriz* and K colors from Peacock et al. (2010) and the spectroscopic metallicities of Perrett et al. (2002). In total, we obtained 127 matches between the old confirmed GCs sample in Fig. 1 and the reddening values of Sect. 2.4, which is the final sample for the fittings of the correlations between metallicities and *ugrizK* colors. In order to thoroughly study the correlations with these photometry, we investigated all the fifteen different colors, for each of which, we plot the linear fitting between the color and metallicities with Eq.(1) in Fig. 4. Similar to Table 1, the intercede a, slope b and the correlation coefficients r are summarized in Table 2. Apparently, all the correlation coefficients (r) are high $(r > 0.7)$, suggesting the *ugriz*K colors are very metal-sensitive. The lowest correlation coefficient is $r_{(i-z)} = 0.701$ while the highest one is $r_{(u-\mathrm{K})} = 0.845$, which might be due to $(u{-}\mathrm{K})_0$ is the widest wavelength coverage color and most absorption lines are included in this range. Whilst, for the $(i-z)_0$ color, the absorption line number should be the least.

It is interesting that Peng et al. (2006) studied the correlation of [Fe/H] and the $(g-z)_0$ for 95 GCs from Milky Way, M87 and M49, and they found that the correlation is very likely nonlinear. Instead, they used a broken linear relation to fit their data. However, such fitting also suffers from scatter and the constraint is not very robust. In fact, we cannot tell which fitting (either the linear or the nonlinear) is significantly better than the other from Fig. 4. In this case, our purpose is to find the metal-sensitive colors and thus the one-order approximation is sufficient.

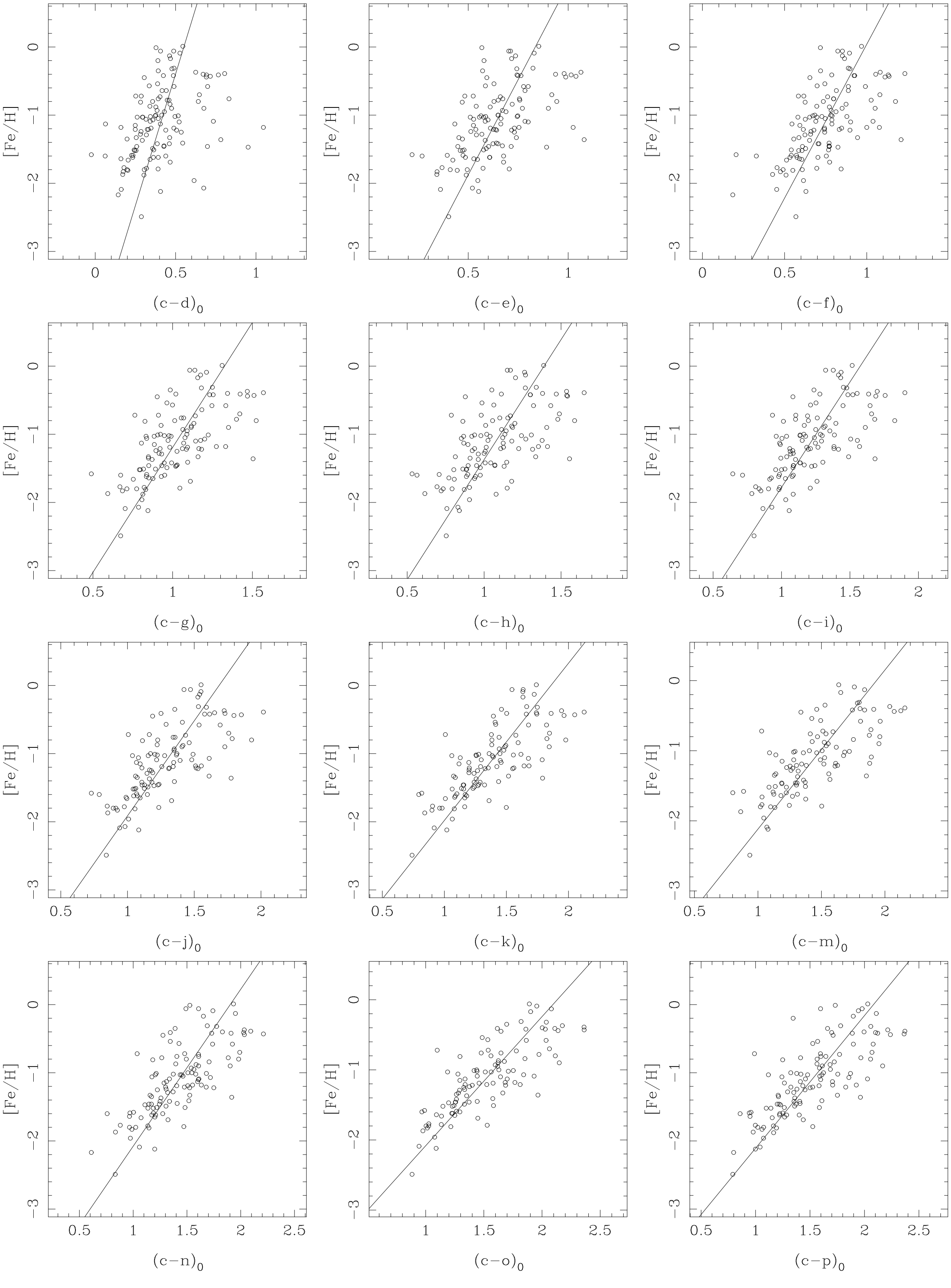
[Fe/H]
0
−1
−2
−3
(c−d)$_0$
0
0.5
1
(c−e)$_0$
0.5
1
(c−f)$_0$
0
0.5
1
(c−g)$_0$
0.5
1
1.5
(c−h)$_0$
0.5
1
1.5
(c−i)$_0$
0.5
1
1.5
2
(c−j)$_0$
0.5
1
1.5
2
(c−k)$_0$
0.5
1
1.5
2
(c−m)$_0$
0.5
1
1.5
2
(c−n)$_0$
0.5
1
1.5
2
2.5
(c−o)$_0$
1
1.5
2
2.5
(c−p)$_0$
0.5
1
1.5
2
2.5

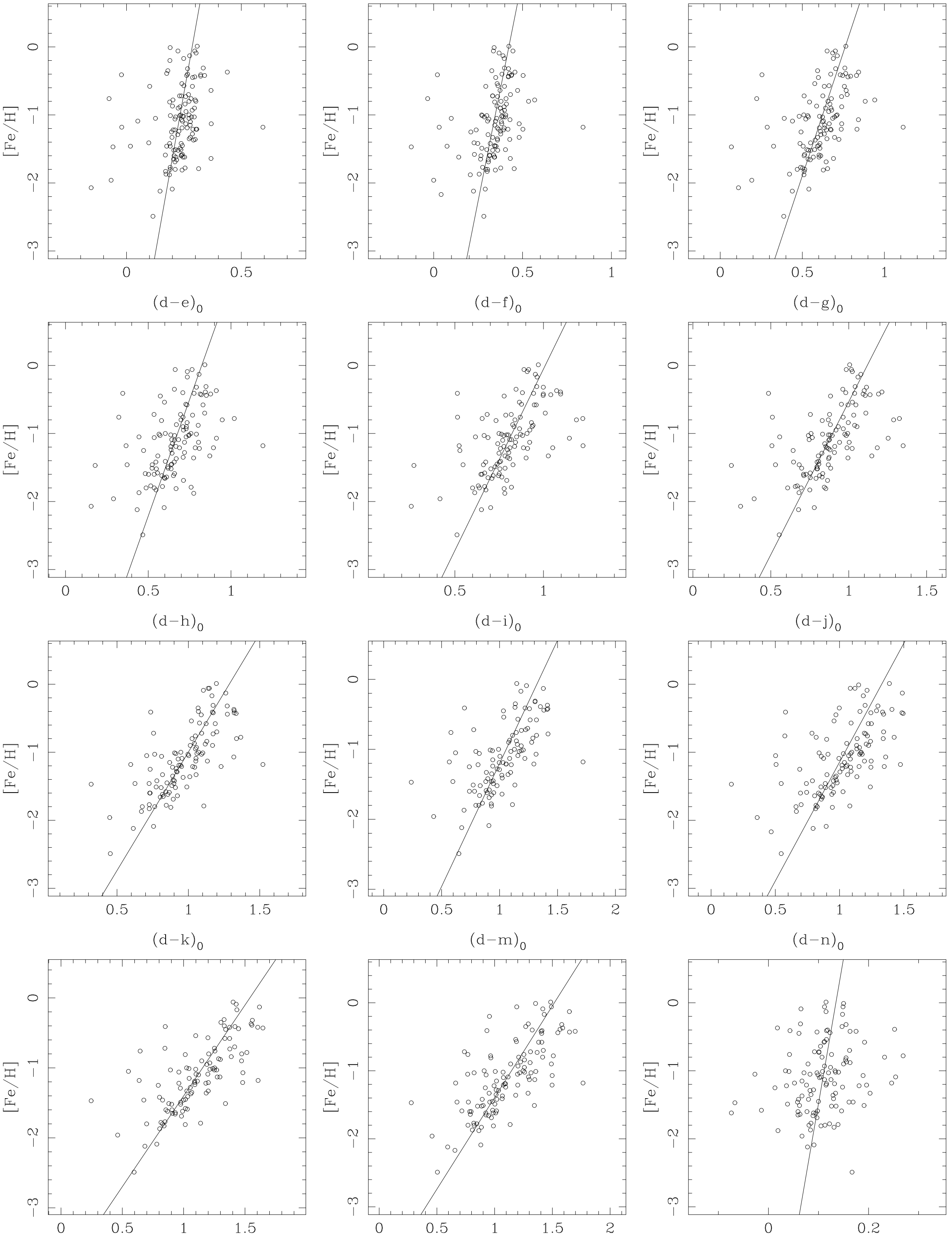
[Fe/H]
0
−1
−2
−3
(d−e)$_0$
0
0.5
(d−f)$_0$
0
0.5
1
(d−g)$_0$
0
0.5
1
(d−h)$_0$
0
0.5
1
(d−i)$_0$
0.5
1
(d−j)$_0$
0
0.5
1
1.5
(d−k)$_0$
0.5
1
1.5
(d−m)$_0$
0
0.5
1
1.5
2
(d−n)$_0$
0
0.5
1
1.5
(d−o)$_0$
0
0.5
1
1.5
(d−p)$_0$
0
0.5
1
1.5
2
(e−f)$_0$
0
0.2

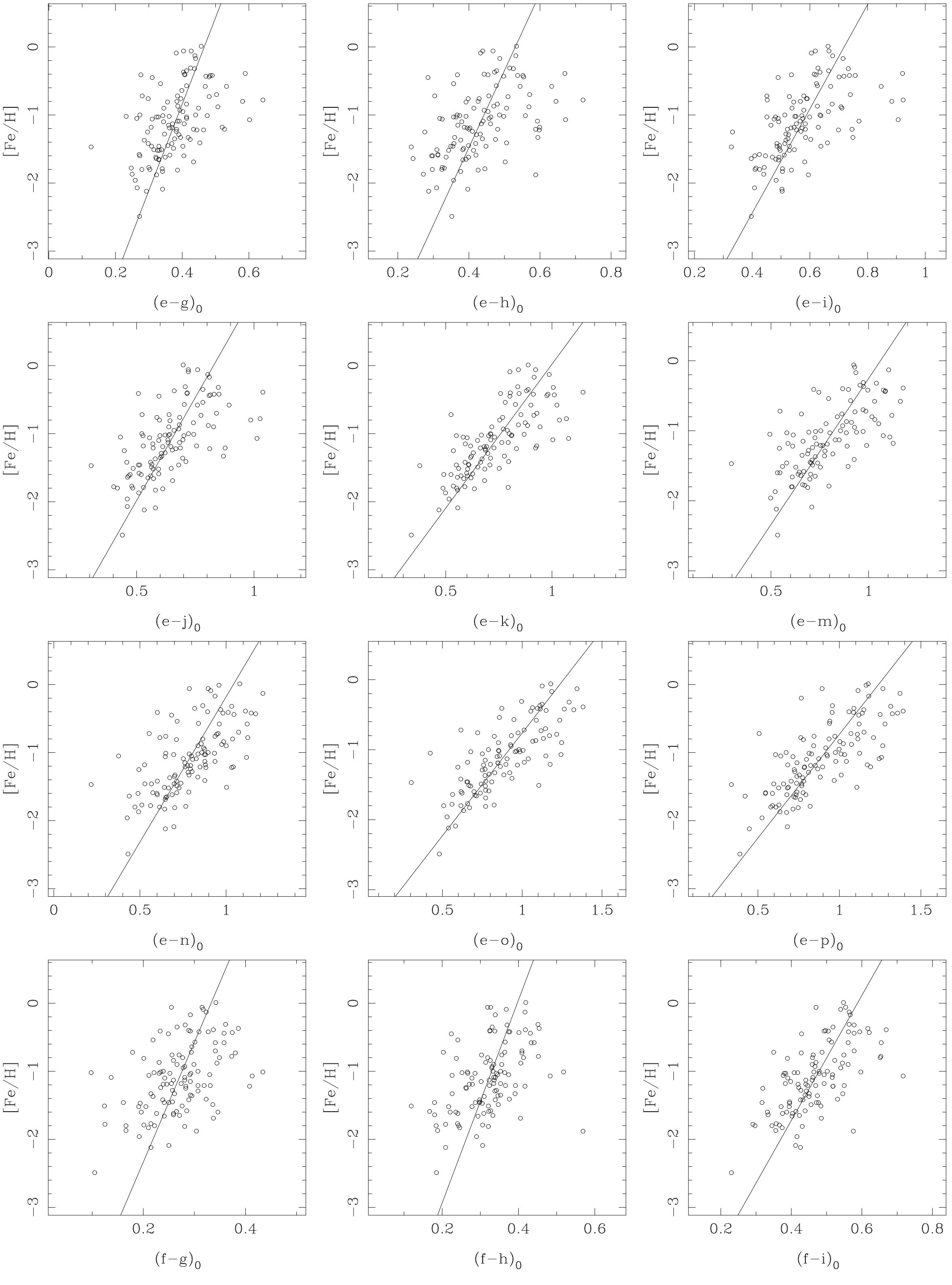
[Fe/H]
0
−1
−2
−3
(e−g)$_0$
0
0.2
0.4
0.6
(e−h)$_0$
0.2
0.4
0.6
0.8
(e−i)$_0$
0.2
0.4
0.6
0.8
1
(e−j)$_0$
0.5
1
(e−k)$_0$
0.5
1
(e−m)$_0$
0.5
1
(e−n)$_0$
0
0.5
1
(e−o)$_0$
0.5
1
1.5
(e−p)$_0$
0.5
1
1.5
(f−g)$_0$
0.2
0.3
0.4
(f−h)$_0$
0.2
0.4
0.6
(f−i)$_0$
0.2
0.4
0.6
0.8

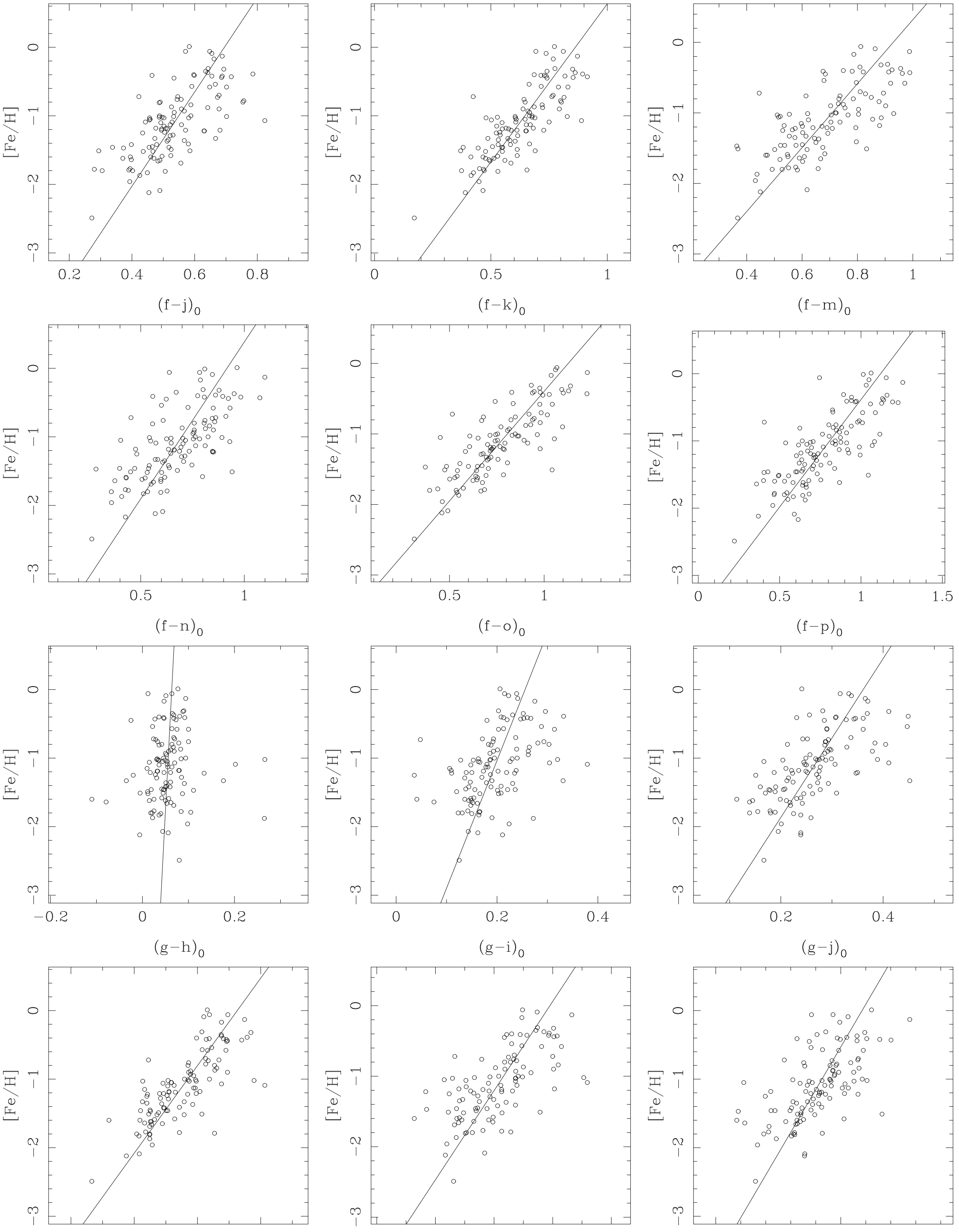
[Fe/H]
0
−1
−2
−3
0.2
0.4
0.6
0.8
(f−j)$_0$
0
0.5
1
(f−k)$_0$
0.4
0.6
0.8
1
(f−m)$_0$
0.5
1
(f−n)$_0$
0.5
1
(f−o)$_0$
0
0.5
1
1.5
(f−p)$_0$
−0.2
0
0.2
(g−h)$_0$
0
0.2
0.4
(g−i)$_0$
0.2
0.4
(g−j)$_0$
0
0.2
0.4
0.6
(g−k)$_0$
0
0.2
0.4
0.6
0.8
(g−m)$_0$
0
0.5
(g−n)$_0$

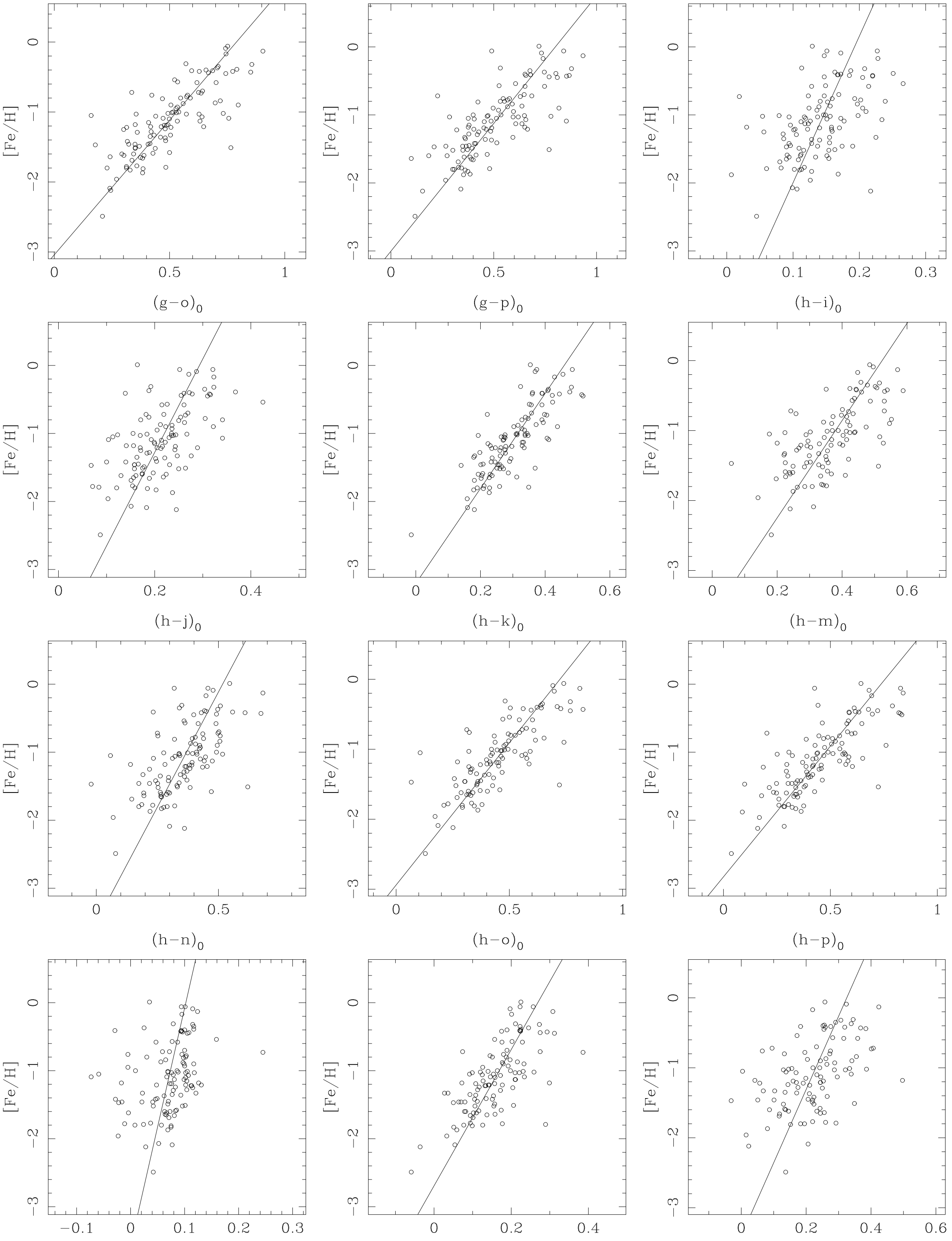
[Fe/H]
(g−o)$_0$
(g−p)$_0$
(h−i)$_0$
(h−j)$_0$
(h−k)$_0$
(h−m)$_0$
(h−n)$_0$
(h−o)$_0$
(h−p)$_0$
(i−j)$_0$
(i−k)$_0$
(i−m)$_0$
0
−1
−2
−3

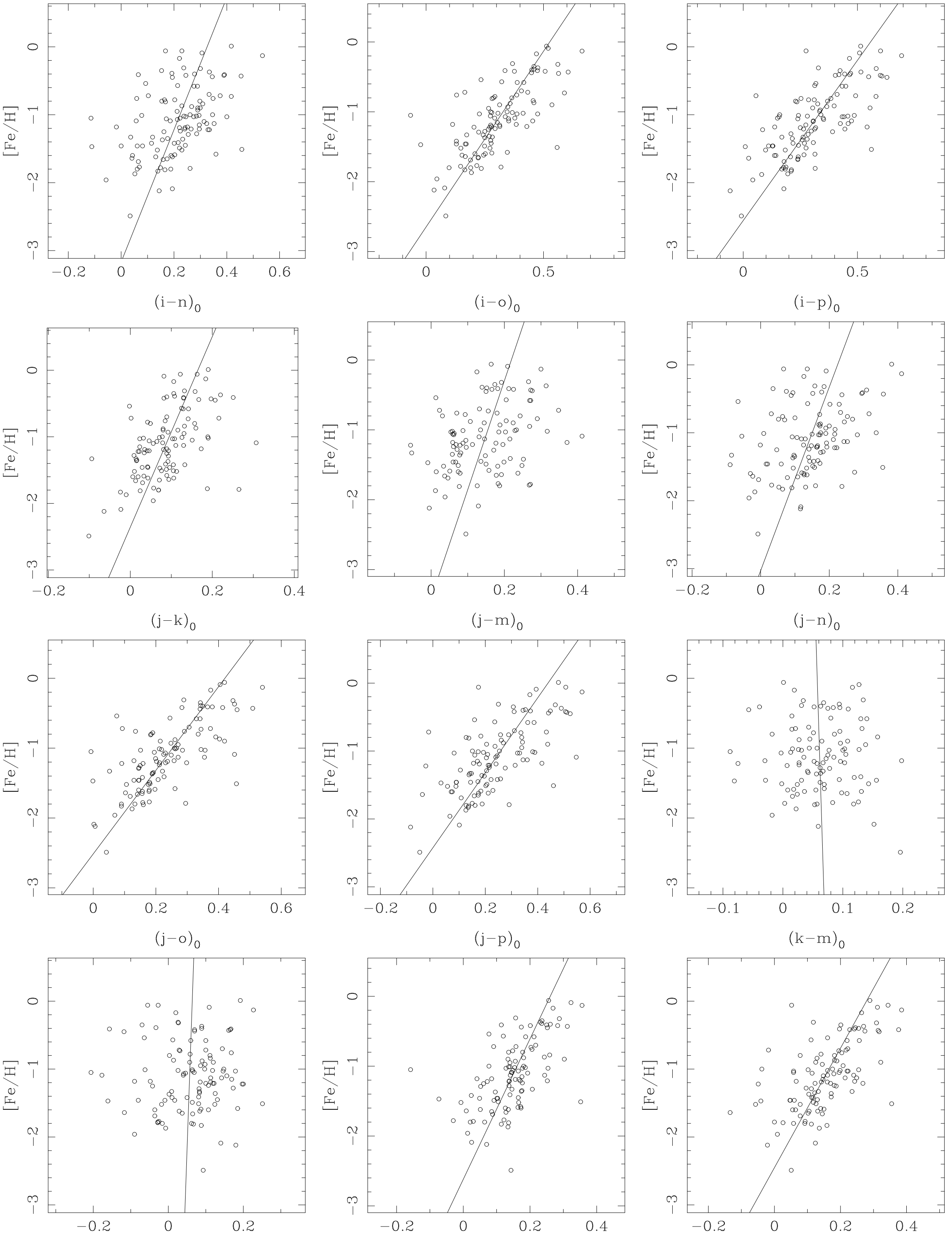
[Fe/H]
0
−1
−2
−3
(i−n)$_0$
(i−o)$_0$
(i−p)$_0$
(j−k)$_0$
(j−m)$_0$
(j−n)$_0$
(j−o)$_0$
(j−p)$_0$
(k−m)$_0$
(k−n)$_0$
(k−o)$_0$
(k−p)$_0$
−0.2
−0.1
0
0.1
0.2
0.4
0.5
0.6

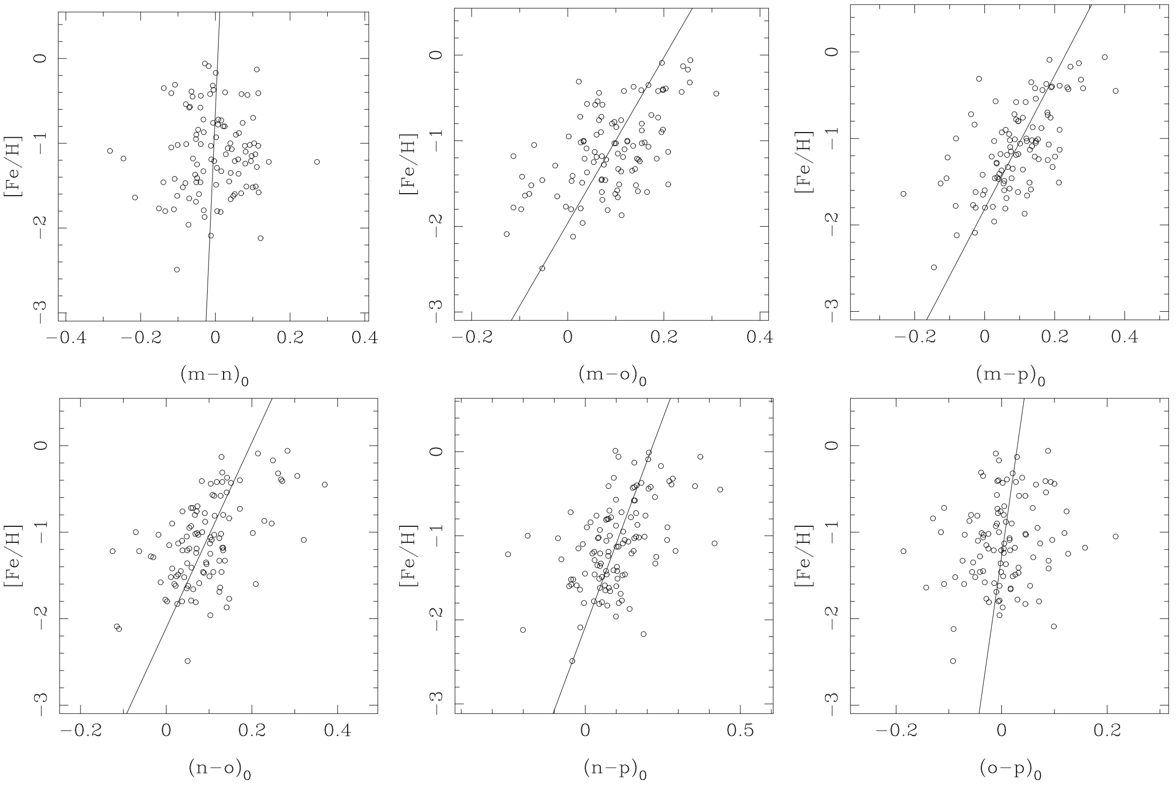
[Fe/H]
0
−1
−2
−3
−0.4
−0.2
0
0.2
0.4
(m−n)$_0$
(m−o)$_0$
(m−p)$_0$
(n−o)$_0$
(n−p)$_0$
0.5
(o−p)$_0$

Table 1: The correlation coefficients of observational spectroscopic metallicities from Perrett et al. (2002) and BATC intrinsic colors. $(x-y)_0 = a + b$[Fe/H].

BATC colors	a	b	r	N
$(c-d)_0$	0.551 ± 0.035	0.130 ± 0.029	0.383	121
$(c-e)_0$	0.836 ± 0.030	0.179 ± 0.024	0.563	119
$(c-f)_0$	0.991 ± 0.033	0.221 ± 0.027	0.607	118
$(c-g)_0$	1.325 ± 0.037	0.273 ± 0.030	0.653	114
$(c-h)_0$	1.390 ± 0.041	0.284 ± 0.033	0.627	113
$(c-i)_0$	1.575 ± 0.042	0.323 ± 0.034	0.668	113
$(c-j)_0$	1.686 ± 0.043	0.359 ± 0.035	0.702	111
$(c-k)_0$	1.859 ± 0.044	0.433 ± 0.037	0.754	109
$(c-m)_0$	1.934 ± 0.050	0.441 ± 0.041	0.726	104
$(c-n)_0$	1.902 ± 0.047	0.434 ± 0.039	0.724	115
$(c-o)_0$	2.131 ± 0.050	0.543 ± 0.041	0.791	107
$(c-p)_0$	2.083 ± 0.050	0.514 ± 0.041	0.759	117
$(d-e)_0$	0.286 ± 0.020	0.053 ± 0.016	0.290	120
$(d-f)_0$	0.423 ± 0.024	0.076 ± 0.020	0.333	119
$(d-g)_0$	0.761 ± 0.030	0.138 ± 0.025	0.465	115
$(d-h)_0$	0.823 ± 0.031	0.146 ± 0.025	0.478	114
$(d-i)_0$	1.010 ± 0.031	0.187 ± 0.025	0.575	114
$(d-j)_0$	1.119 ± 0.036	0.223 ± 0.030	0.584	112
$(d-k)_0$	1.286 ± 0.034	0.287 ± 0.028	0.700	110
$(d-m)_0$	1.342 ± 0.045	0.285 ± 0.037	0.601	105
$(d-n)_0$	1.328 ± 0.044	0.286 ± 0.036	0.596	116
$(d-o)_0$	1.540 ± 0.047	0.385 ± 0.038	0.699	108
$(d-p)_0$	1.517 ± 0.043	0.371 ± 0.035	0.699	118
$(e-f)_0$	0.135 ± 0.012	0.023 ± 0.010	0.212	117
$(e-g)_0$	0.466 ± 0.016	0.079 ± 0.013	0.492	115
$(e-h)_0$	0.531 ± 0.019	0.088 ± 0.016	0.466	114
$(e-i)_0$	0.719 ± 0.021	0.130 ± 0.017	0.576	114
$(e-j)_0$	0.827 ± 0.025	0.165 ± 0.020	0.616	112
$(e-k)_0$	0.995 ± 0.025	0.236 ± 0.020	0.747	110
$(e-m)_0$	1.061 ± 0.032	0.240 ± 0.027	0.665	105
$(e-n)_0$	1.043 ± 0.032	0.234 ± 0.027	0.636	115
$(e-o)_0$	1.259 ± 0.035	0.340 ± 0.029	0.756	108
$(e-p)_0$	1.240 ± 0.034	0.328 ± 0.028	0.733	117

Table 1: Continued.

BATC color	a	b	r	N
$(f-g)_0$	0.333 ± 0.013	0.057 ± 0.010	0.458	114
$(f-h)_0$	0.397 ± 0.015	0.067 ± 0.013	0.449	113
$(f-i)_0$	0.587 ± 0.015	0.109 ± 0.013	0.634	112
$(f-j)_0$	0.695 ± 0.018	0.145 ± 0.015	0.679	111
$(f-k)_0$	0.863 ± 0.019	0.217 ± 0.016	0.800	110
$(f-m)_0$	0.929 ± 0.025	0.221 ± 0.021	0.721	105
$(f-n)_0$	0.916 ± 0.028	0.219 ± 0.023	0.671	115
$(f-o)_0$	1.128 ± 0.028	0.322 ± 0.023	0.802	108
$(f-p)_0$	1.121 ± 0.030	0.313 ± 0.024	0.768	116
$(g-h)_0$	0.064 ± 0.011	0.008 ± 0.009	0.084	113
$(g-i)_0$	0.256 ± 0.012	0.054 ± 0.010	0.458	113
$(g-j)_0$	0.361 ± 0.013	0.086 ± 0.010	0.626	112
$(g-k)_0$	0.526 ± 0.015	0.157 ± 0.013	0.767	110
$(g-m)_0$	0.591 ± 0.023	0.158 ± 0.019	0.641	105
$(g-n)_0$	0.585 ± 0.023	0.161 ± 0.019	0.619	112
$(g-o)_0$	0.790 ± 0.025	0.260 ± 0.020	0.782	108
$(g-p)_0$	0.800 ± 0.026	0.266 ± 0.022	0.761	112
$(h-i)_0$	0.193 ± 0.010	0.046 ± 0.008	0.490	112
$(h-j)_0$	0.293 ± 0.012	0.073 ± 0.010	0.575	111
$(h-k)_0$	0.459 ± 0.012	0.143 ± 0.010	0.813	109
$(h-m)_0$	0.524 ± 0.019	0.144 ± 0.015	0.677	104
$(h-n)_0$	0.517 ± 0.022	0.148 ± 0.018	0.608	112
$(h-o)_0$	0.723 ± 0.023	0.246 ± 0.019	0.782	107
$(h-p)_0$	0.737 ± 0.025	0.260 ± 0.020	0.775	113
$(i-j)_0$	0.102 ± 0.010	0.029 ± 0.008	0.322	111
$(i-k)_0$	0.269 ± 0.012	0.100 ± 0.010	0.690	109
$(i-m)_0$	0.325 ± 0.021	0.096 ± 0.017	0.481	104
$(i-n)_0$	0.325 ± 0.024	0.103 ± 0.020	0.444	112
$(i-o)_0$	0.527 ± 0.023	0.199 ± 0.019	0.714	107
$(i-p)_0$	0.542 ± 0.024	0.212 ± 0.020	0.710	112
$(j-k)_0$	0.165 ± 0.014	0.070 ± 0.011	0.516	109
$(j-m)_0$	0.219 ± 0.021	0.064 ± 0.017	0.343	105
$(j-n)_0$	0.224 ± 0.021	0.074 ± 0.017	0.381	111

Table 1: Continued.

BATC color	a	b	r	N
$(j-o)_0$	0.420 ± 0.020	0.167 ± 0.016	0.706	108
$(j-p)_0$	0.439 ± 0.023	0.181 ± 0.019	0.673	110
$(k-m)_0$	0.057 ± 0.013	-0.004 ± 0.011	-0.033	104
$(k-n)_0$	0.064 ± 0.020	0.006 ± 0.017	0.036	110
$(k-o)_0$	0.261 ± 0.017	0.100 ± 0.014	0.580	106
$(k-p)_0$	0.279 ± 0.018	0.114 ± 0.015	0.600	109
$(m-n)_0$	0.006 ± 0.021	0.010 ± 0.017	0.058	105
$(m-o)_0$	0.203 ± 0.018	0.103 ± 0.015	0.573	105
$(m-p)_0$	0.235 ± 0.019	0.129 ± 0.016	0.634	104
$(n-o)_0$	0.196 ± 0.017	0.093 ± 0.014	0.534	108
$(n-p)_0$	0.210 ± 0.021	0.101 ± 0.017	0.479	115
$(o-p)_0$	0.030 ± 0.015	0.023 ± 0.012	0.186	107

Table 2: The correlation coefficients of the observational spectroscopic metallicities from Perrett et al. (2002) and SDSS *ugriz* and K colors from Peacock et al. (2010). $(x-y)_0 = a + b[\mathrm{Fe/H}]$.

*ugriz*K colors	a	b	r	N
$(g-i)_0$	1.137 ± 0.022	0.248 ± 0.018	0.775	127
$(g-\mathrm{K})_0$	1.439 ± 0.055	0.620 ± 0.043	0.828	96
$(g-r)_0$	0.743 ± 0.015	0.149 ± 0.012	0.740	127
$(g-z)_0$	1.375 ± 0.029	0.342 ± 0.023	0.796	127
$(i-\mathrm{K})_0$	0.316 ± 0.039	0.374 ± 0.030	0.786	96
$(i-z)_0$	0.238 ± 0.011	0.093 ± 0.008	0.701	127
$(r-i)_0$	0.394 ± 0.009	0.099 ± 0.007	0.770	127
$(r-\mathrm{K})_0$	0.705 ± 0.045	0.472 ± 0.035	0.808	96
$(r-z)_0$	0.632 ± 0.017	0.193 ± 0.014	0.785	127
$(u-g)_0$	1.739 ± 0.031	0.309 ± 0.025	0.753	122
$(u-i)_0$	2.874 ± 0.046	0.559 ± 0.037	0.807	122
$(u-\mathrm{K})_0$	3.160 ± 0.080	0.927 ± 0.062	0.845	92
$(u-r)_0$	2.480 ± 0.039	0.459 ± 0.032	0.797	122
$(u-z)_0$	3.112 ± 0.052	0.651 ± 0.042	0.816	122
$(z-\mathrm{K})_0$	0.094 ± 0.034	0.292 ± 0.027	0.750	96

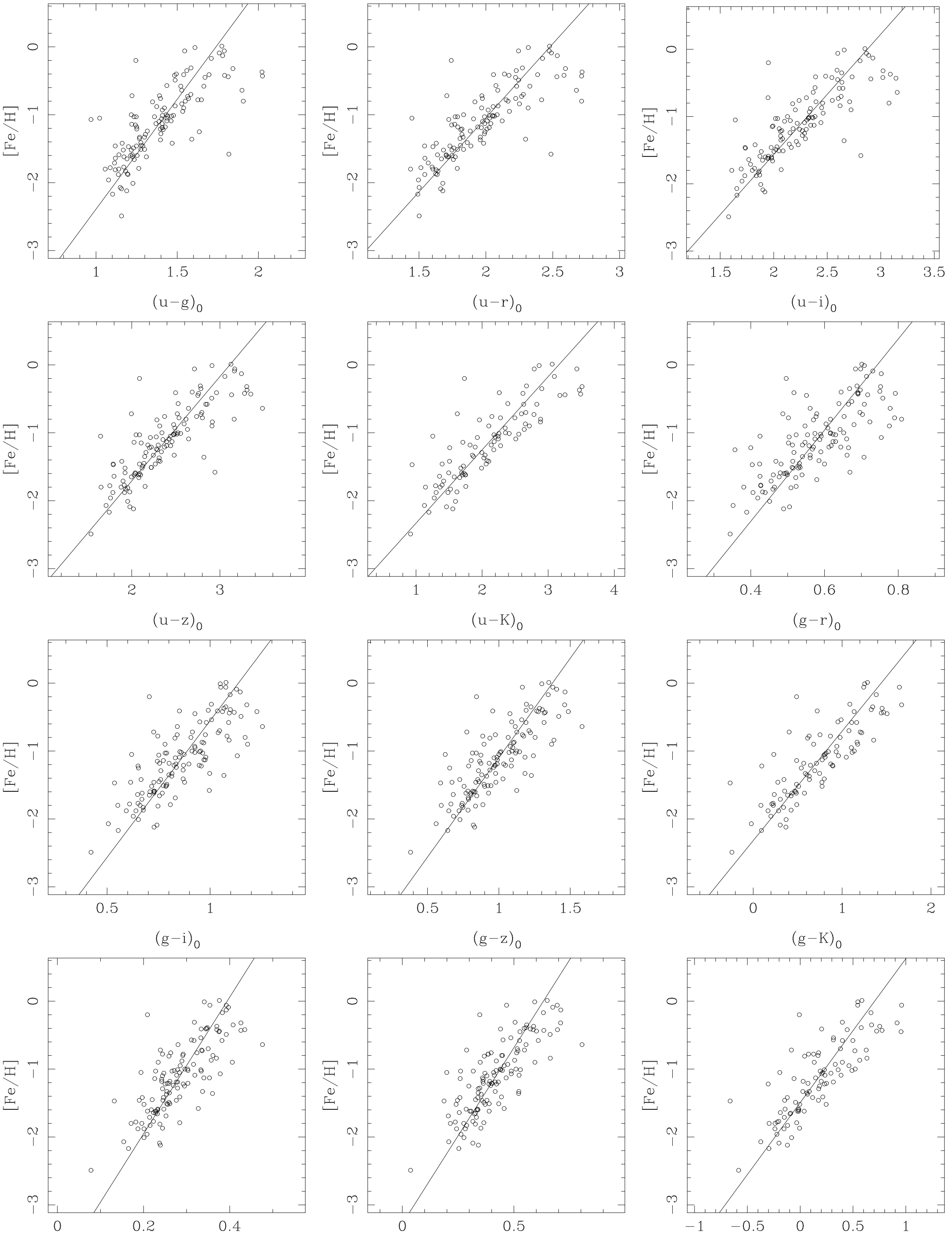
[Fe/H]
0
−1
−2
−3
1
1.5
2
(u−g)$_0$
1.5
2
2.5
3
(u−r)$_0$
1.5
2
2.5
3
3.5
(u−i)$_0$
2
3
(u−z)$_0$
1
2
3
4
(u−K)$_0$
0.4
0.6
0.8
(g−r)$_0$
0.5
1
(g−i)$_0$
0.5
1
1.5
(g−z)$_0$
0
1
2
(g−K)$_0$
0
0.2
0.4
(r−i)$_0$
0
0.5
(r−z)$_0$
−1
−0.5
0
0.5
1
(r−K)$_0$

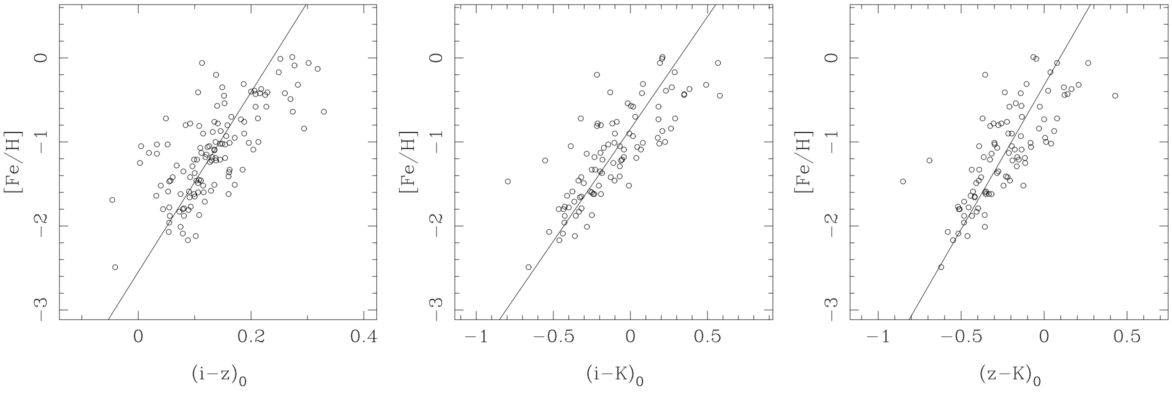
[Fe/H]
0
−1
−2
−3
0
0.2
0.4
(i−z)$_0$
[Fe/H]
0
−1
−2
−3
−1
−0.5
0
0.5
(i−K)$_0$
[Fe/H]
0
−1
−2
−3
−1
−0.5
0
0.5
(z−K)$_0$

4. Summary

Our work provides the most metal-sensitive colors of M31 GCs which could be utilized for roughly estimating the metallicity of GCs from their colors. The observational spectroscopic metallicities applied in our analysis were from Perrett et al. (2002) and the colors are derived from BATC photometry and Peacock et al. (2010).

First, we performed the photometry with BATC archival images from c to p band, covering the wavelength from $\sim$ 4,000 to $\sim$ 10,000 Å and obtained the BATC colors for 123 confirmed old GCs. The reddening values for the color corrections are from Fan et al. (2008) and Barmby et al. (2000). For the thorough study, all the seventy-eight different BATC colors are used for the correlation analysis. Our fitting result shows that correlation coefficients of 23 colors $r > 0.7$. Especially, for the colors $(f-k)_0$, $(f-o)_0$, $(h-k)_0$, the correlation coefficients $r > 0.8$. Meanwhile, the correlation coefficients approach zero for $(g-h)_0$, $(k-m)_0$, $(k-n)_0$, $(m-n)_0$, which can be explained by lacking absorption lines.

Further, we also fitted the correlations of metallicity and $ugriz$K colors for the 127 old confirmed GCs with the photometry from Peacock et al. (2010). Similarly, all the fifteen colors are utilized for analysis. The fitting result indicates that all these colors are metal-sensitive with correlation coefficients $r > 0.7$. In particular, $(u-\mathrm{K})_0$ is the most metal-sensitive color while $(i-z)_0$ is the metal-nonsensitive color.

We are very grateful to an anonymous Referee for her/his useful comments and suggestions. This research was supported by the Chinese National Natural Science Foundation through Grant Nos. 10873016, 10803007, 10778720, 10633020, 10673012 and by National Basic Research Program of China (973 Program) No. 2007CB815403. Z.F. thanks the Young Researcher Grant of National Astronomical Observatories, Chinese Academy of Sciences.

REFERENCES

Barmby, P., Huchra, J. P., Brodie, J. P., Forbes, D. A., Schroder, L. L., Grillmair, C. J. 2000, AJ, 119, 727

Battistini, P., Bònoli, F., Braccesi, A., Fusi Pecci, F., Malagnini, M. L., Marano, B. 1980, A&AS, 42, 357

Battistini, P., Bònoli, F., Braccesi, A., Federici, L., Fusi Pecci, F., Marano, B., Börngen, F. 1987, A&AS, 67, 447

Battistini, P., Bònoli, F., Casavecchia, M., Ciotti, L., Federici, L., & Fusi Pecci, F. 1993, A&A, 272, 77

Bertin, E., Arnouts, S. 1996, A&AS, 117, 393

Brodie, J. P., Huchra, J. P. 1990, AJ, 362, 503

Caldwell, N., Harding, P., Morrison, H., Rose, J. A., Schiavon, R., Kriessler, J. 2009, AJ, 137, 94

Crampton, D., Cowley, A. P., Schade D., Chayer, P. 1985, ApJ, 288, 494

Fan, X. H., et al., 1996, AJ, 112, 628

Fan, Z., Ma, J., de Grijs, R., Yang, Y., Zhou, X. 2006, MNRAS, 371, 1648

Fan, Z., Ma, J., de Grijs, R., Zhou, X. 2008, MNRAS, 385, 1973

Fan, Z., Ma, J., Zhou, X. 2009, RAA, 9, 993

Galadí-Enríquez, D., Trullols, E., & Jordi, C. 2000, A&AS, 146,169

Galleti, S., Federici, L., Bellazzini, M., Fusi Pecci, F., Macrina, S. 2004, A&A, 416, 917

Galleti, S., Federici, L., Bellazzini, M., Buzzoni, A., Fusi Pecci, F. 2006, A&A, 456, 985

Galleti, S., Bellazzini, M., Federici, L., Buzzoni, A., Fusi Pecci, F. 2007, A&A, 471, 127

Hubble, E. 1932, ApJ, 76, 44

Huxor, A. P., Tanvir, N. R., Ferguson, A. M. N., Irwin, M. J., Ibata, R., Bridges, T., Lewis, G. F. 2008, MNRAS, 385, 1989

Jiang, L., Ma, J., Zhou, X., Chen, J., Wu, H., Jiang, Z. 2003, AJ, 125, 727

Kim, S., et al., 2007, AJ, 134, 706

Landolt, A. U., 1983, AJ, 88, 439

Landolt, A. U., 1992, AJ, 104, 340

Ma, J., et al., 2006, ApJ, 659, 359

Ma, J, et al., 2009, AJ, 137, 4884

Mackey, A. D., Huxor, A., Ferguson, A. M. N., Tanvir, N. R., Irwin, M., Ibata, R., Bridges, T., Johnson, R. A., Lewis, G. 2006, ApJ, 653, 105

Macri L. M., 2001, ApJ, 549, 721

Massey, P., Olsen, K. A. G., Hodge, P. W., Strong, S. B., Jacoby, G. H., Schlingman, W., Smith, R. C. 2006, AJ, 131, 2478

Oke, J. B., & Gunn, J. E. 1983, ApJ, 266, 713

Peacock, M. B., Maccarone, T. J., Knigge, C., Kundu, A., Waters, C. Z., Zepf, S. E., Zurek, D. R. 2010, MNRAS, 402, 803

Peng, E. W., Jordán, A., Côté, P., Blakeslee, J. P., Ferrarese, L., Mei, S., West, M. J., Merritt, D., Milosavljević, M., Tonry, J. L. 2006, ApJ, 639, 95

Perrett, K. M., Bridges, T. J., Hanes, D. A., Irwin, M. J., Brodie, J. P., Carter, D., Huchra, J. P., Watson, F. G. 2002,AJ, 123, 2490

Racine, R. 1991, AJ, 101, 865

Sargent, W. L. W., Kowal, C. T., Hartwick, F. D. A., van den Bergh, S. 1977, AJ, 82, 947

Stanek, K. Z., Garnavich, P. M. 1998, ApJ, 503, 131

Vetesnik, M. 1962, Bull. Astr. Inst. Czechoslovakia, 13, 180

Wang, S., Fan, Z., Ma, J., de Grijs, R., Zhou, X. 2010, AJ, 139, 1438

Worthey, G., 1994, ApJS, 95,107

Yan, H. J., et al., 2000, PASP, 112, 691

Zhou, X., et al., 2003, A&A, 397, 361

This preprint was prepared with the AAS LaTeX macros v5.2.